

# “Endothelial antibody factory” at the Blood Brain Barrier: novel approach to therapy of neurodegenerative diseases

**Renald thinard**

ALSaTECH

**Attila Farkas**

Inst. of Biophysics, Biological Res. Centre, Eötvös Lorand Research Network (ELKH)

**Marta Halasa**

Laboratory of Molecular Oncology and Innovative Therapies, Military Institute of Medicine

**Melanie Chevalier**

ALSaTECH

**Klaudia Brodaczewska**

Laboratory of Molecular Oncology and Innovative Therapies, Military Institute of Medicine

**Aleksandra Majewska**

Laboratory of Molecular Oncology and Innovative Therapies, Military Institute of Medicine

**Robert Zdanowski**

Laboratory of Molecular Oncology and Innovative Therapies, Military Institute of Medicine

**Maria Paprocka**

Hirszfeld Inst Immunol & Expt Therapy, Polish Acad Sci.

**Joanna Rossowska**

Hirszfeld Inst Immunol & Expt Therapy, Polish Acad Sci.

**Lam Duc**

Inst. of Biophysics, Biological Res. Centre, Eötvös Lorand Research Network (ELKH)

**Ruth Greferath**

ALSaTECH

**Istvan Krizbai**

Inst. of Biophysics, Biological Res. Centre, Eötvös Lorand Research Network (ELKH)

**Fred Leuven**

LEGTEGG, Katholieke Universiteit Leuven

**Claudine Kieda**

Centre national de la Recherche Scientifique <https://orcid.org/0000-0002-7573-029X>

**Claude Nicolau** (✉ [cnicolau4@gmail.com](mailto:cnicolau4@gmail.com))

Friedman School of Nutrition Science and Policy

## Article

### Keywords:

**Posted Date:** March 1st, 2022

**DOI:** <https://doi.org/10.21203/rs.3.rs-1325519/v1>

**License:**  This work is licensed under a Creative Commons Attribution 4.0 International License.

[Read Full License](#)

---

# Abstract

Phase III clinical trials of immunotherapies against Alzheimer's disease have failed to hit major endpoints. Despite the high doses administered, small fractions of injected monoclonal antibodies cross the blood brain barrier (BBB), likely resulting in an antibody concentration in the brain parenchyma that is too low for a therapeutic effect. Here we report a novel approach to circumvent this obstacle. Leveraging the homing properties of endothelial progenitor cells (EPCs) to reach impaired BBB, we transfected ex vivo EPCs with vectors encoding anti- $\beta$ -amyloid and anti-TDP-43 antibody fragments (Fabs). The expressed Fabs retained the ability to bind to, and extensively solubilize,  $\beta$ -amyloid and TDP-43 aggregates. Immunofluorescence studies showed that when injected into mice, the transfected EPCs homed to the BBB where they adhered, integrated, and expressed Fabs which localized in the brain parenchyma and perivascular space. This approach can be optimized and developed as a possible cell-based gene and immunotherapy.

## Introduction

Neurodegenerative disorders including Alzheimer's disease (AD) and Amyotrophic Lateral Sclerosis (ALS) are accepted to be caused by the accumulation of misfolded proteins in the brain [1-3]. Monoclonal antibodies (mAbs) have been developed to clear misfolded proteins and their aggregates [4-6]. To date, all Phase-III clinical trials have been unsuccessful in hitting major endpoints. Despite the high doses administered, only a small fraction crosses the blood brain barrier (BBB) (less than 1%) [7,8]. The BBB is an extremely efficient filter, not permitting its crossing by 98% of the therapeutic agents tried to date [9,10]. It is a continuous endothelial layer lining the brain microvessels that has sealed cell-to-cell contacts and is sheathed by neural vascular cells and perivascular astrocytic end-feet [10]. Breakdown of the BBB, observed in a number of neurodegenerative diseases, does not favor crossing by therapeutic antibodies, proteins and peptides for several reasons clearly described by Sweeney et al. [10]. Successful delivery of therapeutic agents across the BBB requires structurally healthy blood vessels, normal vascularization, adequate blood flow and recruitment of solute carrier-mediated transport or receptor-mediated transcytosis systems [10]. Endothelial progenitor cells (EPCs) have been shown to repair damaged Blood-Spinal cord Barrier with beneficial therapeutic consequences [11].

Several studies have documented the regenerative potential of EPCs, and their capacity to sustain a functional vascular system, which is vital to transporting nutrients, signaling molecules, and cells to the site of tissue injury [12-14]. Research from the last decade suggests that EPC's regenerative ability may be effective in more than just vascular tissue [15,16]. Indeed, the features of EPCs, such as migration, homing and vasculogenesis indicate their potential for use in transplantation or cell-gene therapy for various diseases [17-19].

Here we report pre-clinical data on the development of a novel approach using ex-vivo transfected EPCs as cellular producers of anti-TDP-43 and anti- $\beta$ -amyloid antibody fragments (Fabs) as depicted on **figure 1**. Most neurodegenerative diseases are typified by neuroinflammation leading to BBB breakdown. Their

homing properties make EPCs, injected systemically, migrate into the BBB in response to local hypoxia. The locally secreted Fabs then migrate to the brain parenchyma, as shown in this paper.

## Results

We have raised antibodies against specific sequences of  $\beta$ -amyloid ( $\beta$ -amyloid 1-16) and TDP-43 (TDP-43 311-344), both effectively dissolving *in vitro* aggregates of the respective proteins. Previous studies with intact antibodies have shown a solubilization of  $\beta$ -amyloid of about 80% [20]. We prepared Fab fragments of the antibodies that retain the capacity of solubilization of the aggregates in dose-dependent manner (shown for anti-TDP-43 in **Fig. 2**). The protein sequence of the active Fab fragments allowed us to build expression vectors containing the respective Fab encoding sequences as well as the insulin gene sequence to facilitate the export of the expressed protein [21].

Prior to transfecting endothelial progenitor MAgEC cells with the anti-TDP-43 and anti- $\beta$ -amyloid Fab encoding vectors, we validated transfected endothelial progenitor MAgEC cells for their capacity to produce and secrete exogenous proteins after transfection, using the soluble enhanced Green Fluorescent Protein (s-EGFP) as proof of concept. Different clones were selected by resistance to hygromycin from the transfected MAgEC 10.5 cell line, and tested by flow cytometry (**Fig. 3 a, c**), in comparison with non-producing clone as control (**Fig. 3 b**). The stability of expression and secretion of s-EGFP by the transfected clones was confirmed over several passages (data not shown) and was proportional to seeded cell number (**Fig. S1**).

Transient transfection with anti- $\beta$ -amyloid Fab encoding vector using electroporation resulted in the production and secretion of Fabs, solubilizing the  $\beta$ -amyloid aggregates as described by Heller, Thinard et al. [21].

To be able to track the cells *in vivo* for longer duration experiments, the endothelial progenitor MAgEC 10.5 were transduced to express the red fluorescent protein, tdTomato (named MAgEC 10.5 RT) before to be transfected with the Fab encoding vectors. We went on to stably transfect these MAgEC 10.5 RT cells with the vectors constructed for the anti- $\beta$ -amyloid and anti-TDP-43 Fabs. The supernatants of selected clones were analyzed in the aggregation assay (shown for anti- $\beta$ -amyloid in **Fig.4 a**). The results demonstrated effective solubilization of the aggregates with the supernatants from MAgEC 10.5 anti-TDP-43 cells compared to non-transfected MAgEC 10.5 RT as negative control (no Fab production). The production and secretion of Fabs by the clones were also demonstrated by Western Blot (shown for anti-TDP-43 in **Fig. 4 b**). We concluded that the cell culture-produced and secreted Fabs retained their ability to recognize amyloid- $\beta$ , or TDP-43.

Cytofluorometric analyses of biological markers of the MAgEC 10.5 anti-TDP-43 cells (**Fig. 4 c**) demonstrated that the MAgEC 10.5 anti-TDP-43 cells producing and secreting the anti-TDP-43 Fab retained the expression profile of the non-transfected MAgEC 10.5 RT (**Fig. 4 d**). Moreover, the transfected cells were shown to adhere to the murine brain endothelial cells (MBrMEC) thus confirming their potential to recognize, *in vivo*, the BBB endothelial cells (**Fig. 4 e**).

MAGEC 10.5 immortalized endothelial precursor cells fluorescently labeled using Cell Tracker Red were injected into the common carotid artery of adult wild type BALB/c mice. Their brains were sectioned at multiple time points after injection. We could detect *in vivo* MAGEC 10.5 cells localizing in the brain, as soon as 4 hours after injection (**Fig. 5 a**). Identification of the astrocytes, the pericytes, the vessel wall endothelial cells and extracellular matrix collagen IV, permitted to localize the endothelial progenitors MAGEC 10.5 inside the vessels together with their insertion in the BBB. (**Fig. 5 b**). Immunolabeling for PECAM-1 and laser scanning fluorescent microscopy was used to outline brain capillary microvessels around the fluorescent EPCs. Following shortly after injections, EPCs imaged in brain sections appear to fill the capillary lumen. As early as 28 hours after injection, EPCs were observed to become located flattening against and adhering to the vessel walls (**Fig. 5 c**).

Next, for longer duration experiments, MAGEC 10.5 were transduced to express the red fluorescent protein, tdTomato (named MAGEC 10.5 RT), and similarly injected into BALB/c mice. Cells were observed 7 days post injection for staining for the tight junction protein marker claudin 5. These results showed the formation of tight junctions between the injected MAGEC 10.5 RT as well with unlabeled resident endothelial cells (**Figure 5 d and e**). We concluded that the injected MAGEC 10.5 RT were integrating into the capillary bed.

We went on to test our hypothesis that EPCs can be used as vectors for treating neurological disorders by integrating into the vasculature and secreting therapeutic molecules. Therefore, MAGEC 10.5 RT cells were further modified to also express the anti-TDP-43 Fab (cells named MAGEC 10.5 RT anti-TDP-43). Following characterization of the cells and carotid injection into BALB/c mice, immunolabeling was used to localize the MAGEC 10.5 RT anti-TDP-43 cells and the anti-TDP-43 Fab expressed in relation to the brain microvasculature. The anti-TDP-43 Fab was detected in EPCs located in the brain vasculature 7 days after injection (**Fig. 6 a**). Furthermore, anti-TDP-43 Fabs were also observed outside PECAM-1 labeled microvessels that contained red fluorescent EPCs expressing this Fab (**Fig. 6 b**).

To test whether the Fab localized into the perivascular space and penetrated into the brain parenchyma, we immunolabeled astrocytic endfeet that ensheath the microvasculature by its specific marker aquaporin-4. We observed a distinct localization of the Fabs along the aquaporin-4 stained endfeet (**Fig. 6 c**). From these images it was not possible to differentiate luminal and the abluminal sides of astrocytic endfeet even using super-resolution microscopy (**Fig. 6 d**). Nevertheless, we observed sites where the Fabs were clearly localized in the brain parenchyma, past the aquaporin-4 signal. Of interest, we further noted that the extravascular anti-TDP-43 Fab appeared co-located with tdTomato originating from MAGEC 10.5 RT anti-TDP-43 cells, suggesting vesicular localization (**Fig. 6 e**).

## Discussion

The approach to a therapy of neurodegenerative diseases described in this work adds to the already existing therapeutical uses of EPC [19, 21, 22] by using transfected EPCs that express active antibody fragments. This system has a dual function: (1) the EPCs themselves repair the damaged BBB occurring

in both ALS and AD –, and (2) transfected EPCs secrete, at the BBB, the anti-TDP-43 and anti- $\beta$ -amyloid Fabs capable of solubilizing the aggregates of TDP-43 and  $\beta$ -amyloid. The results presented show that it is possible to establish a production of antibody fragments by transfected EPCs, and that these Fabs bind to aggregates of TDP-43 and  $\beta$ -amyloid, solubilizing a significant fraction of them in a concentration-dependent manner. Moreover, the transfected EPCs 7-days post-injection became stained for the marker claudin 5, indicating the formation of tight junctions between the injected MAgEC 10.5 RT and unlabeled resident endothelial cells. Thus, it clearly appears that the injected cells were integrated in the capillary bed.

The experimental results further showed localization of the Fabs in the perivascular space and in the brain parenchyma. Immunolabeling of the astrocytes end-feet with its specific marker aquaporin-4 showed a clear localization of the Fabs in the brain parenchyma, past the aquaporin signal. The results obtained demonstrate that antibodies produced at the BBB by EPCs transfected with our expression vectors are capable of penetrating the brain parenchyma. The results suggest that the EPCs could be transfected not only with vectors expressing antibody fragments, but with vectors expressing other exogenous proteins that are normally blocked by the BBB.

In summary, *ex vivo* transfection of endothelial progenitor cells with expression vectors led to the production of antibody fragments (Fabs) retaining their ability to recognize TDP-43 and  $\beta$ -amyloid aggregates. When such cells were injected into mice, they were detected at the BBB, where they integrated, continuing Fab production. Immunofluorescence studies showed that some of the injected cells form tight junctions among them and with the unlabeled resident endothelial cells. The natural repair process of vessels in pathologic angiogenesis-induced damage is the recruitment of EPCs from the bone marrow or mobilization upon paracrine signaling of endothelial progenitors from vicinal tissues [19, 23]. Combining the BBB-repairing by the EPCs with the production *in situ* of antibodies or Fabs directed against TDP-43 or  $\beta$ -amyloid might lead to a cell-based gene and immunotherapy of neurodegenerative and many other diseases.

## Methods

### 1. Preparation of the antigens.

Briefly,  $\beta$ -Amyloid and TDP-43 antigens were prepared as previously described [20]. In the case of  $\beta$ -Amyloid antigen, the peptide used was palmitoylated peptide 1–16. For the TDP-43 antigen, the peptide used was non-palmitoylated peptide 311-344.

### 2. Immunizations, antibody fragments (Fabs) cloning and production.

The immunizations were done by Absolute Antibody (Oxford, UK). To raise antibodies against our peptides, C57BL/6 mice were immunized for 98 days with liposomes presenting the antigen at their surface. Their spleen B-cells were then fused with P3-X63-Ag8 myeloma line to obtain Hybridomas. Hybridomas were then sequenced by whole transcriptome shotgun sequencing. After identification of the

mature VH and VL regions sequences, they were subcloned in expression vectors to be expressed in Human Embryonic Kidney 293 (HEK293) cells. Cells were transiently transfected with heavy and light chain expression vectors and cultures for a further 6 to 14 days. Cultures were harvested and the Fabs were purified using affinity chromatography and analyzed for purity by SDS-PAGE. The quantity of Fabs were finally quantified by ELISA.

### **3. Plasmids.**

To create pSF-CAG.InsSP-EGFP, the OG4678 vector (OxGene, Oxford, UK), encoding the CAG promoter, was used as parent vector. PCR was performed to append the human insulin signal peptide to EGFP. Restriction and ligation were performed with the EGFP PCR product and OG4678 to create the final construct for expression and secretion of EGFP. pl.DualCAG.Hygro.cAb2789 encodes both chains of an anti- $\beta$ Amyloid Fab with optimized peptide signals driven by dual CAG promoters. In addition, a His tag is included to simplify the screening of the Fab production. pl.DualCAG.Hygro.cAb2789 was created with pSF-CAG.InsSP-GFP as parent vector. The parent vector was restricted and was subsequently ligated with a restricted DNA fragment corresponding to the ubiquitin promoter, a downstream hygromycin resistance marker for cell selection, and a polyadenylation sequence. PCR was performed to append optimized peptide signals to both chains of the anti- $\beta$ -Amyloid Fab encoding sequences (CH1-VH and CL-VL). In addition, a 10-His tag encoding sequence was added to the heavy chain encoding sequence. Finally, the fragments were subcloned into the parent vector with CAG promoters for both chains to create the final vector expressing and secreting the anti- $\beta$ Amyloid Fab. Using the same method, pl.DualCAG.Hygro.cAb2508 was synthesized and encodes both chains of an anti TDP-43 Fab. pSF-CAG.InsSP-GFP, pl.DualCAG.Hygro.cAb2789 and pl.DualCAG.Hygro.cAb2508 were verified with restriction digests and Sanger sequencing. All plasmids were commercially prepared with endotoxin levels confirmed to be <100 EU/mg (OxGene, Oxford, UK) and diluted to 2 mg/ml in physiological saline.

### **4. Cell line.**

MAGEC 10.5 cells (murine endothelial progenitor cell line) [Kieda C et al (2011) Human and murine stem-cell lines: models of endothelial cell precursors / *Fasc. European Patent EP 2 524 030 B1*] were grown as previously described by Collet et al. [19] in Opti-MEM containing 2% FBS (Gibco, ThermoFisher Scientific, Irvine, CA, USA) at 37 °C with 5% CO<sub>2</sub>.

### **5. Cell transduction with tdTomato lentiviral expression vectors.**

To establish the MAGEC 10.5 cell line displaying tdTomato expression, the third-generation lentiviral system consisting of pMDLg/pRRE, pRSV-Rev, pMD2.G (a gift from Didier Trono (Addgene plasmid # 12251, 12253, 12259)) and expression plasmids pLV[3Exp]-EF1A->{tdTomato}:IRES:Puro (VectorBuilder) were used. Lentiviral vectors were produced using Lenti-X™ 293T cell line (Clontech, USA) according to the protocol described by Rossowska et al. [25]. Stable MAGEC 10.5/tdTomato cell line, renamed MagEC 10.5 RT, was obtained after selection with puromycin (10  $\mu$ g/mL, from Sigma-Aldrich). Transduction efficacy

was analyzed for their fluorescence emission of the tdTomato protein in cells by flow cytometry (FACS Aria, Becton Dickinson).

## 6. Cell transfection and cloning.

MAgEC 10.5 RT was seeded at 30 000 cells per well in a 12 wells plate, allowed to adhere for 12 hours, and then the medium was exchanged with serum-free OptiMEM. After 6 hours, cells were transfected with Lipofectamine 2000 and Fabs-encoding vectors (pl.DualCAG.Hygro.cAb2789 or pl.DualCAG.Hygro.cAb2508) according to the manufacturer's instructions. Cells were transfected and kept for further 12 hours in a serum-free medium. After 12 hours, the hygromycin selection (125 µg/ml) was made. After 24 hours of hygromycin selection, the medium was removed and replaced with the fresh one. The medium was changed every two days in two weeks. After two weeks, the hygromycin-resistant colonies were observed. To obtain proper clones, the cells were detached and seeded at 96 wells plate (1 cell/per well). Selected clones were checked for Fab secretion using western blotting technique.

## 7. Western blot His-tagged Fab.

MAgEC 10.5 clones were cultured for 3-5 days Using OPTI MEM with 2% FBS and 125 ug/ml hygromycin. When the cells reached 90-100% confluence, they were detached by Accutase and counted. Cells were centrifuged, washed with PBS and RIPA buffer with protease inhibitors added. Cells lysates were stored at -20 °C. Then, the lysates were centrifuged at 4000×g for 10 mins at 4°C. Protein concentration was quantified using a Pierce™ BCA Protein Assay Kit (ThermoFisher Scientific). Cell lysates were solubilized in 4×Laemmli sample buffer and boiled for 5 mins at 100°C. 15-20 µg of protein extracts were separated on 10% SDS-PAGE (First: 10 minutes, 100V, next: about 60 minutes, 180V at 4°C) and transferred onto the nitrocellulose membrane. Following the transfer, the membrane was blocked with blocking buffer (5% nonfat dried milk in TBS/0.1% Tween-20 (TBST)) for 1 hr at RT and incubated overnight at 4°C with primary antibodies. On the following day, the membrane was washed and then incubated with appropriate horseradish peroxidase-labeled secondary antibodies for 1 hr at RT. Finally, target proteins were visualized using Western Blotting Luminol Reagent (Santa Cruz Biotechnology) according to the manufacturer's protocol. β-actin was used as a loading control. For MAgECs supernatants, the protocol was the same except for estimating the protein concentration.

Primary antibodies	Cat. No.
Anti-Histag Chimeric	Merck, SAB5600096
Anti-Mouse IgG (Fab specific)	ThermoFisher, 31413
Secondary antibodies	
Anti-Histag Chimeric secondary	Merck, A1293
Rabbit anti-Goat IgG (H+L) secondary	ThermoFisher, 81-1620

## 8. Assessment of surface markers using flow cytometry.

To evaluate expression of surface markers, cells from culture were detached with Acutase Solution (Biolegend, USA). Cell suspension was washed with PBS and incubated with TruStain FcX™ PLUS (anti-mouse CD16/32) (#156603 Biolegend, USA) 10 minutes on ice to block non-specific binding of immunoglobulin to the Fc receptors. The reagent was used according to the manufacturer's protocol 0.25 µg per 10<sup>6</sup> cells in a 100 µl PBS. The cells were then centrifuged, and staining was performed using 10<sup>5</sup> cells for single marker. Antibodies and isotopic controls used in experiment listed in Table 1; in concentration recommended by manufacturer in 100µl Stain Buffer (FBS) (BD Pharmingen™, USA). Incubation was continued for 30 minutes on ice. After staining cells were washed twice with 300 µl PBS. Finally, 50 µl of cell suspension in Stain Buffer (FBS) was prepared and cells were analyzed by flow cytometry using CYTOFLEX software v.2.3.0.84 (Becton Dickinson, USA). The lower threshold was used to exclude debris and live cells with gating (10<sup>4</sup> cells), according to forward scatter (FSC) × side scatter (SSC) and only singlets were analyzed. Due to the red color of MAgEC RT cells, auto-fluorescence in different channels was checked. APC and Pacific Blue450 were selected as the most useful (the weakest auto-fluorescence). Data were presented as delta MFI to reduce the impact of auto-fluorescence.

Table 1 List of antibodies:

Antibody	Catalog number	Details
CD34	152207 (Biolegend)	Rat IgG2a Brilliant Violet 421™
CD45	103111(Biolegend)	Rat IgG2b APC
UEA-1	DL-1069 (Vector Laboratories)	DyLight649 labeling
Isotype Control Antibody	400511 (Biolegend)	Rat IgG2a APC
Isotype Control Antibody	400611(Biolegend)	Rat IgG2b APC

## 9. Solubilization capacity of $\beta$ -amyloid or TDP-43 aggregates.

Reaction tubes containing 30 µg of  $\beta$ -Amyloid 1–42 protein (Bachem, Bubendorf, Switzerland) or 30µg of TDP-43 protein (LS-Bio, Seattle, Washington, USA) in 10µl of PBS, pH 7.4 (Gibco), were incubated for 1 week at 37°C. Aggregation was measured by the thioflavin T (ThT)-binding assay, in which the dye's fluorescence emission intensity reflects the degree of fibrillar aggregation. Disaggregation was followed after addition of purified antibodies, Fab or supernatants from Fab producing-clones to the preformed fibers (10 µl each). The purified IgG, Fab and an irrelevant control antibody (mouse IgG) were used at a final concentration of 1,5 mg/ml. The reaction incubated for 2 days at 37°C. Fluorescence (excitation:450 nm; emission: 482 nm) was measured after addition of 1 ml of ThT (3 µM in 50 mM sodium phosphate buffer, pH 6.0) on Fluoromax4C fluorometer (Horiba, Kyoto, Japan).

## 10. Hypoxia sensitivity of murine brain-derived endothelial cells (MBrMECs) recognition by MAgEC 10.5 RT cell line by adhesion experiment.

The adhesion experiment was performed as previously described [26]. A proportion 1:1 for MAgECs/MBrMECs was used. For hypoxia effect assessment, MBrMECs cells were pre-cultured for 48 hours in a cell incubator (19,5% O<sub>2</sub>) or hypoxia chamber (Biospherix X3 Vivo System, USA) set for a 1% O<sub>2</sub> atmosphere for 72 h to reach confluence. After 72 hours, MAgEC 10.5 RT cells (control and selected clones) were counted and added in suspension at a ratio of 1:1 to MBrMECs monolayers and were incubated for 20 min at RT with gentle rocking. Un-attached cells were washed off with warm medium. The remaining cells were detached with Accutase and analyzed by flow cytometry. The ratio of MAgEC 10.5 RT to MBrMECs was counted based on the number of events detected in PerCP-positive (MAgECs) to PerCP-negative (MBrMECs) gates.

## 11. Animal experiments and immunofluorescence.

All mice were housed and treated in accordance with widely accepted standards, and the protocols were approved by the institutional care and the Regional Animal Health and Food Control Station of Csongrád-Csanád County (permit number: XVI./764/2018).

8–14-week-old BALB/c mice were anesthetized via inhaled isoflurane 4% (v/v) in synthetic air for induction and 1–2% (v/v) for maintenance, using an isoflurane vapourizer (Stoelting). Depth of anesthesia was monitored by toe pinch tests. Endothelial precursor cells (EPC) - 4.10<sup>5</sup> MAgEC 10.5 RT cells labeled with CellTracker Red (C34552, Thermo Fisher) according to the manufacturer's instructions, MAgEC 10.5 RT cells or MAgEC 10.5 RT anti-TDP-43 cells - were injected into the common carotid artery while the external carotid artery was ligated. 4 hours to 7 days later the animals were sacrificed and perfused transcardially with 4 w/w % formaldehyde. Overnight post-fixation with the same fixative was followed by vibratome sectioning to 30 micrometer thickness. The sections were immunolabeled using antibodies Fab (1:200, A1293 Sigma-Aldrich), PECAM-1 (1:100, NB100-2284, Novus Biologicals), claudin 5 (1:200, 35-2500, Invitrogen, Thermo Fisher), aquaporin-4 (1:100, sc-390488, Santa Cruz) and secondary antibodies donkey- $\alpha$ -goat-Alexa+647, donkey- $\alpha$ -rabbit-Alexa+488 donkey- $\alpha$ -mouse-Alexa+488 (1:500, A32849, A32790, A32766, Invitrogen, Thermo Fisher). Syto-13 (1:10000, S7575, Invitrogen) was used as a nuclear counterstain. Immunofluorescence was recorded using a fluorescence microscope (Axiovert Z1, Zeiss) equipped for super-resolution capable laser scanning confocal microscopy (Stedycon, Abberior Instruments).

## 12. Statistical analysis.

The results were analyzed using GraphPad Prism 9.0 software. Data are expressed as mean  $\pm$  standard deviation of the mean ( $\pm$ SD). Statistical differences were considered relevant at  $p < 0.05$  (\*  $p < 0.05$ , \*\*  $p < 0.01$ , \*\*\*  $p < 0.001$ , \*\*\*\*  $p < 0.0001$ ).

## Declarations

Contributions

**RT:** Project management, designed and conducted experiments, Methodology, Validation, Investigations, Formal analysis, Writing, Review & Editing. **A.E.F:** Designed and conducted experiments, Methodology, Investigations, Formal analysis, Writing, Review & Editing. **MH:** Conducted experiments, Validation, Investigations, Methodology. **MC:** Conducted experiments, Validation, Investigations, Methodology. **KB:** Methodology, Investigations, Formal analysis, Validation. **AM:** Conducted experiments, Validation, Investigations, Methodology. **RZ:** Conducted experiments, Validation, Investigations, Methodology. **MP:** Conducted experiments, Methodology, Validation, Investigations. **JR:** Conducted experiments, Methodology, Validation, Investigations. **L.T.D:** Conducted experiments, Methodology, Investigations, Validation. **RG:** Methodology, Resources. **IK:** Designed experiments, Methodology, Editing. **F.V.L:** Methodology, Review & Editing. **CK:** Methodology, Validation, Designed experiments, Writing, Review & Editing. **CN:** Conceptualization, Design of the experiments, Methodology, Validation, Resources, Writing, Review & Editing, Project administration

## Acknowledgements

Stimulating discussions with Prof. I. Rosenberg (Boston, MA) and Prof. D. Riesner (Düsseldorf, Germany) Great and productive work with OXGENE (Oxford, UK) especially Robert Leydon are gratefully acknowledged.

## Competing interests

**RT, MC, RG** are employed by ALSaTECH ; **F.V.L** is a shareholder ; **CN** is a consultant of ALSaTECH.

## References

1. Polymenidou M. and Cleveland D.W., the seeds of neurodegeneration: prion-like spreading in ALS (2011) *Cell*, 147(3):498-508
2. Polymenidou M., and Cleveland D.W., Prion-like spread of protein aggregates in neurodegeneration (2012) *J. Exp. Med.*, 209(5):889-893
3. R. C. Hergesheimer and al., The debated toxic role of aggregated TDP-43 in amyotrophic lateral sclerosis: a resolution in sight? (2019) *Brain*, 142(5):1176-1194
4. Muhs, A. et al., Liposomal vaccines with conformation-specific amyloid peptide antigens define immune response and efficacy in APP transgenic mice (2007) *Proc Natl Acad Sci U S A.* 104:9810-5.
5. Kwong L. K. et al., Novel monoclonal antibodies to normal and pathologically altered human TDP-43 proteins (2014) *Acta Neuropathol Commun*, 2:33
6. Murakami K., Conformation-specific antibodies to target amyloid  $\beta$  oligomers and their application to immunotherapy for Alzheimer's disease (2014) *Biosci Biotechnol Biochem.*, 78(8):1293-305.
7. Thom G. et al., Isolation of blood-brain barrier-crossing antibodies from a phage display library by competitive elution and their ability to penetrate the central nervous system (2018) *MAbs*, 10(2):304-314

8. YuZuchero Y.J. et al., Discovery of Novel Blood Brain Barrier targets to enhance brain uptake of therapeutic antibodies (2016) *Neuron*, volume 89, issue 1 pages 70-82
9. Pardridge, W.M., "Blood Brain Barrier delivery" *Drug Discovery Today*, volume 12, 54-61, 2007
10. Sweeney, M. D. et al., Blood Brain Barrier: From physiology to disease and back, *Physiol. Rev.* 99 (1), 21-78, 2019
11. Garbuzova-Davis S. et al., Human bone marrow endothelial progenitor cell transplantation into symptomatic ALS mice delays disease progression and increases motor neuron survival by repairing blood-spinal cord barrier (2019) *Scientific reports* 9:5280
12. Kalka C. et al., Transplantation of ex vivo expanded endothelial progenitor cells for therapeutic neurovascularization (2000) *Proc. Natl. Acad. Sci. USA* 97:3422-7
13. Kong Z. et al., Endothelial progenitor cells improve functional recovery in focal cerebral ischemia of rat by promoting angiogenesis vis VEGF (2018) *J. Clin. Neurosci.* 55:116-21
14. Collet, G. et al. Trojan horse at cellular level for tumor gene therapies, 525, 208-215, 2013
15. Cao J.P. et al., Autologous transplantation of peripheral blood-derived circulating endothelial progenitor cells attenuates endotoxin-induced acute lung injury in rabbits by direct endothelial repair and indirect immunomodulation (2012) *Anesthesiology* 116:1278-87
16. Kado M. et al., Human peripheral blood mononuclear cells enriched in endothelial progenitor cells via quality and quantity-controlled culture accelerate vascularization and wound healing in porcine wound model (2018) *Cell transplant*, 27:1068-79
17. Suh W. et al., Transplantation of endothelial progenitor cells accelerates dermal wound healing with increased recruitment of monocytes/macrophages and neovascularization (2005) *Stem cells* 23:1571-8
18. Jung K.H. et al., Circulating endothelial progenitor cells in cerebrovascular disease (2008) *J. Clin. Neurol.* 4:139-47
19. Collet, G. et al., Endothelial precursor cell-based therapy to target the pathological angiogenesis and compensate tumor hypoxia (2016) *Cancer Lett.* 370(2):345-57
20. Nicolau, C. et al., A liposome-based therapeutic vaccine against beta-amyloid plaques on the pancreas of transgenic NORBA mice (2002) *Proc Natl Acad Sci U S A.*, 99(4):2332-7
21. Heller L. and Thinard R. et al., Secretion of proteins and antibody fragments from transiently transfected endothelial progenitor cells (2020) *J Cell Mol Med.* 00:1-7
22. Garbuzova-Davis S. et al., Implication of Blood Brain Barrier disruption in ALS (2008) *Amyotrophic Lateral Sclerosis*, 9:375-376
23. Sen S. et al., Endothelial progenitor cells: novel biomarker and promising cell therapy for cardiovascular disease (2011) *Clinical Sciences* 120, 263-283
24. Chopra H. et al., Insights into Endothelial Progenitor Cells: Origin, Classification, Potentials, and Prospects (2018) *Stem Cells Int*, 2018:9847015.

25. Rossowska J. et al., Intratumoral Lentivector-Mediated TGF- $\beta$ 1 Gene Downregulation as a Potent Strategy for Enhancing the Antitumor Effect of Therapy Composed of Cyclophosphamide and Dendritic Cells (2017) *Frontiers in Immunology* Jun 30;8:713
26. Paprocka, M. et al., Flow cytometric assay for quantitative and qualitative evaluation of adhesive interactions of tumor cells with endothelial cells. (2008) *Microvasc Res*;76, 134-138.

## Figures

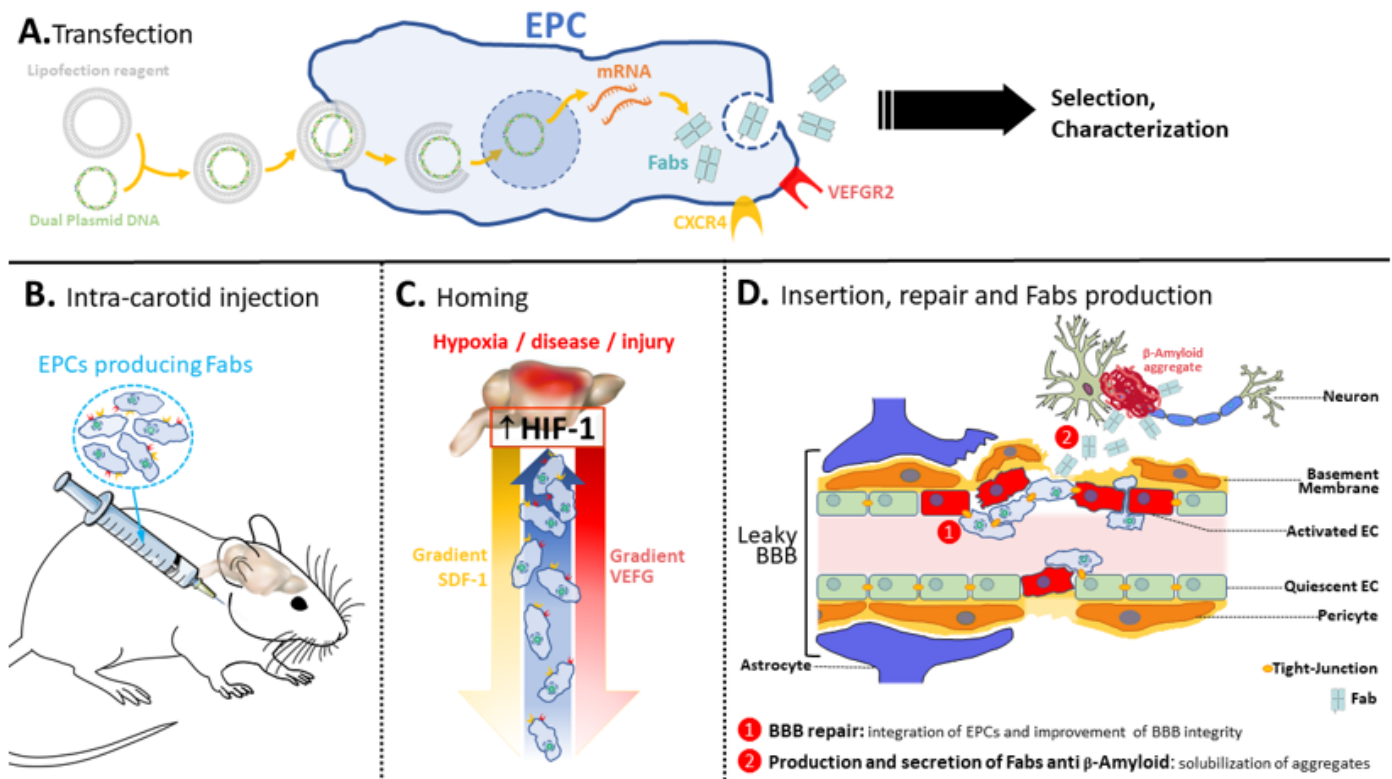


Figure 1

**Therapeutic concept.** Taking AD as example, the strategy is to combine a cell therapy using the EPCs and the immunotherapy with the secretion of anti- $\beta$ -amyloid Fabs. After transfection the Fab producing EPCs are selected and characterized before to be injected in the mice (old or AD mice). The transfected EPCs then home to the brain where they secrete the solubilizing Fabs. This system has a dual function: (1) the EPCs themselves, homing to the brain and integrating the BBB, repair the damaged BBB occurring in AD -, and (2) transfected EPCs secrete, at the BBB, anti- $\beta$ -amyloid Fabs capable of solubilizing the aggregates.

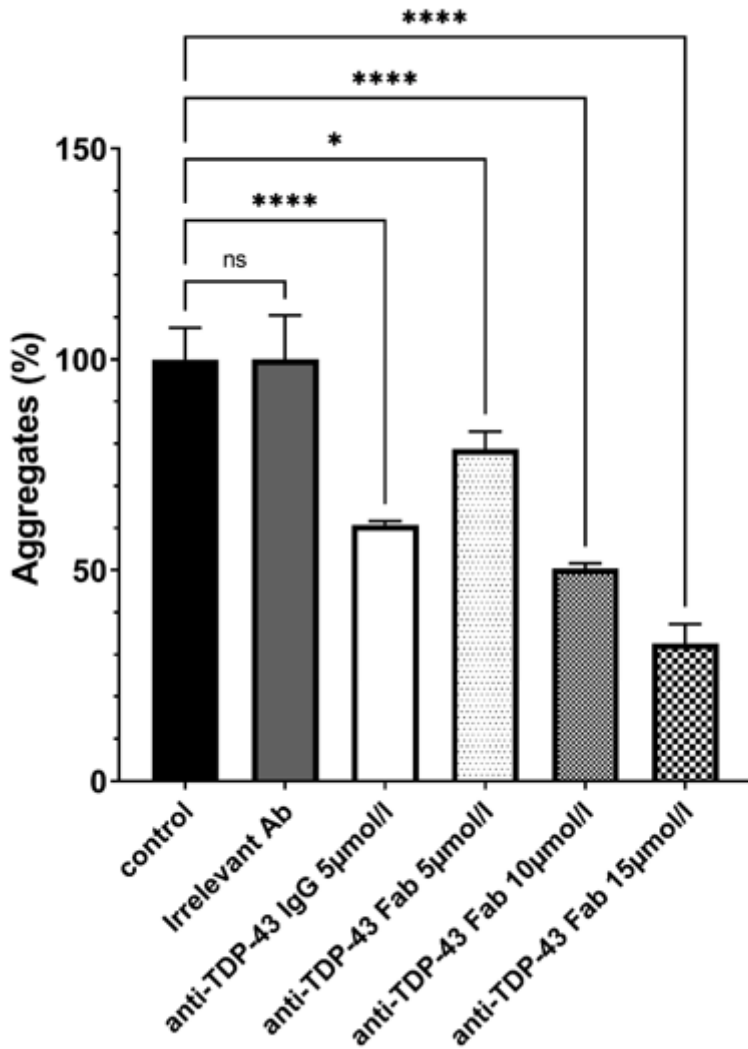
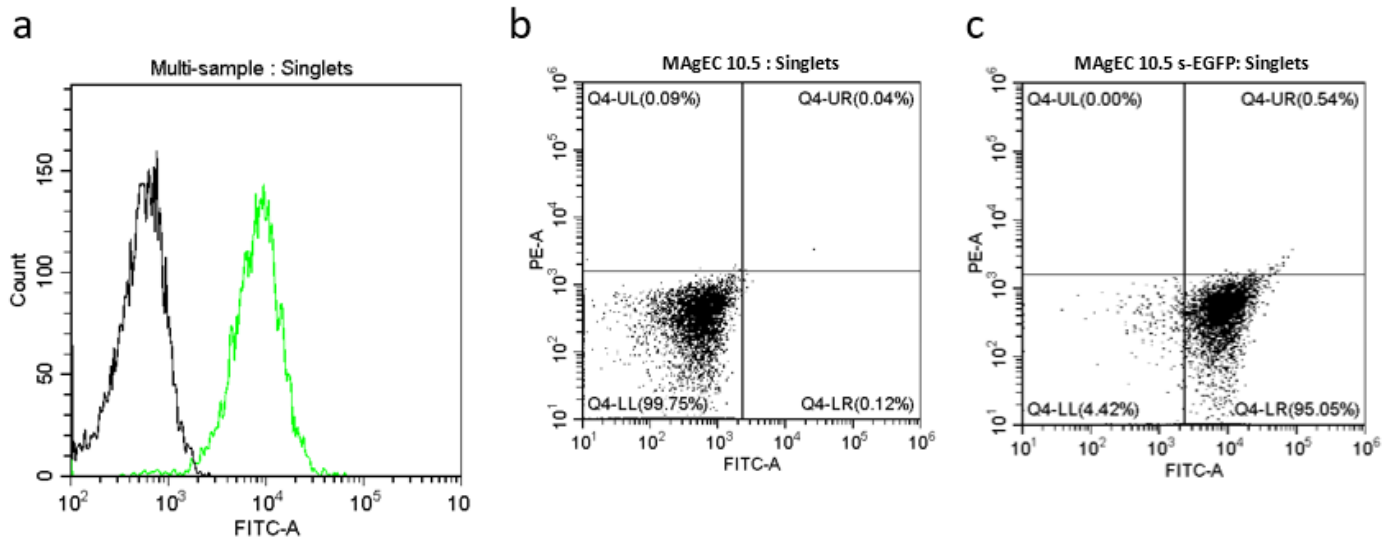


Figure 2

**Characterization of the antibodies and Fab produced by clones.** The solubilization capacity of the purified antibodies was first tested *in vitro* on human TDP-43 aggregates using full size anti TDP-43 IgG or anti-TDP-43 Fab at several concentrations. Several concentrations of Fabs were tested to match molar equivalence (5µmol/l) or mass equivalence (15µmol/l) compared to anti-TDP-43 IgG (used at 5µmol/l). The test was also performed with anti-β-amyloid Fab (data not shown). n=3 per group.



**Figure 3**

**Flow cytometry analysis of the expression of s-EGFP by the transfected MAgEC 10.5 s-EGFP.** Expression of s-EGFP MAgEC 10.5 s-EGFP (a. green line on histogram, dot plot c.) in comparison with non-transfected cells MAgEC 10.5 analyzed as control (a. grey line on histogram, dot plot b.)

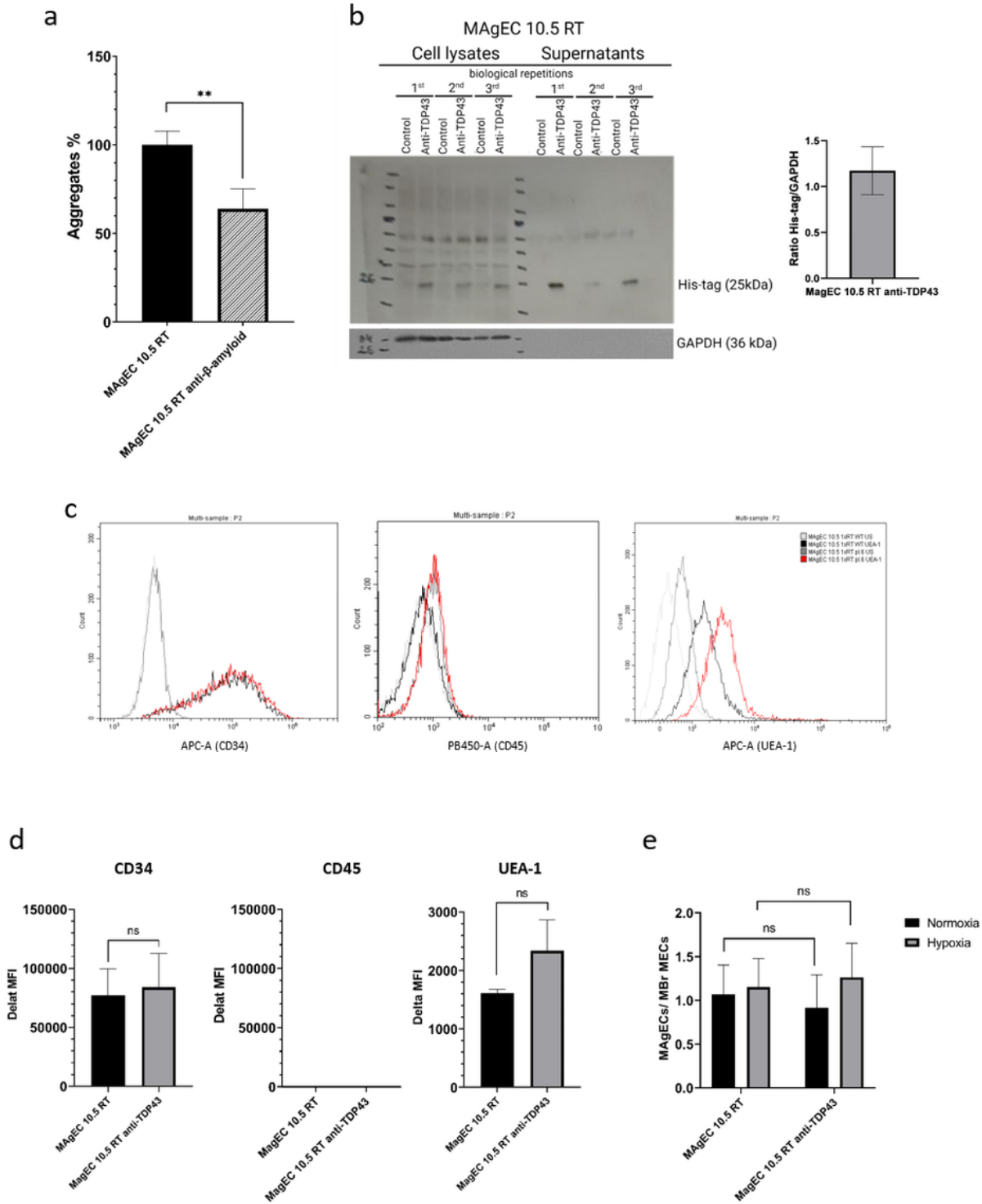


**Figure 4**

**Characterization of the MAgEC 10.5 RT anti-β-amyloid and MAgEC 10.5 RT anti-TDP-43 cells: solubilizing Fab production and cell markers.** **a**, Solubilization capacity of anti-β-amyloid Fabs produced and secreted by the Fab-producing MAgEC 10.5 RT anti-β-amyloid cells. Supernatants from these cells were tested *in vitro* on human β-amyloid aggregates. n=3 per group. **b**, Production and secretion of anti-TDP-43 Fab using Western Blot. Fabs are expressed and secreted by the Fab-producing MAgEC 10.5 RT anti-TDP-43

cells. The cell lysates and equal amount of medium from subconfluent cultures after 72 h of culture were used for analysis. The GAPDH was used as control. The densitometry analysis shows the ratio between His-tag and GAPDH in MAgEC 10.5 RT anti-TDP-43 from cell lysates. n=3. **c**, Flow cytometry analysis of MAgEC 10.5 RT and MAgEC 10.5 RT anti-TDP-43 cells. Grey lines for the 3 cell markers represent the unstained controls for the MAgEC 10.5 RT (light grey) and MAgEC 10.5 RT anti-TDP-43 cells (dark grey), respectively. Black lines represent expression in MAgEC 10.5 RT cells and red ones the expression on MAgEC 10.5 RT anti-TDP-43 cells surface. Both cell lines are CD34+, CD45- and bind UEA-1. **d**, Comparative cell marker expression of MAgEC 10.5 RT and MAgEC 10.5 RT anti-TDP-43 using flow cytometry. The quantitative expression of the markers is expressed in Delta MFI. No difference of expression is observed between the two cell lines confirming that the Fab producing MAgEC 10.5 RT anti-TDP-43 retains the same phenotype. n=3 per group. **e**) Hypoxia sensitivity of murine brain-derived endothelial cells (MBrMECs) recognition by MAgEC 10.5 RT by adhesion experiment. The adhesion experiment was performed in proportion 1:1 for MAgECs/MBrMECs in two conditions: hypoxia (grey bars) or normoxia (black bars). After incubation of the MAgEC 10.5 RT or MAgEC 10.5 RT anti-TDP-43 suspension on MBrMECs layer, un-attached cells are removed and then the ratio of MAgEC 10.5 RT to MBrMECs is counted. MAgEC 10.5 RT anti-TDP-43 cells show no significant difference in adhesion capacity compared to the MAgEC 10.5 RT. n=3 per group.

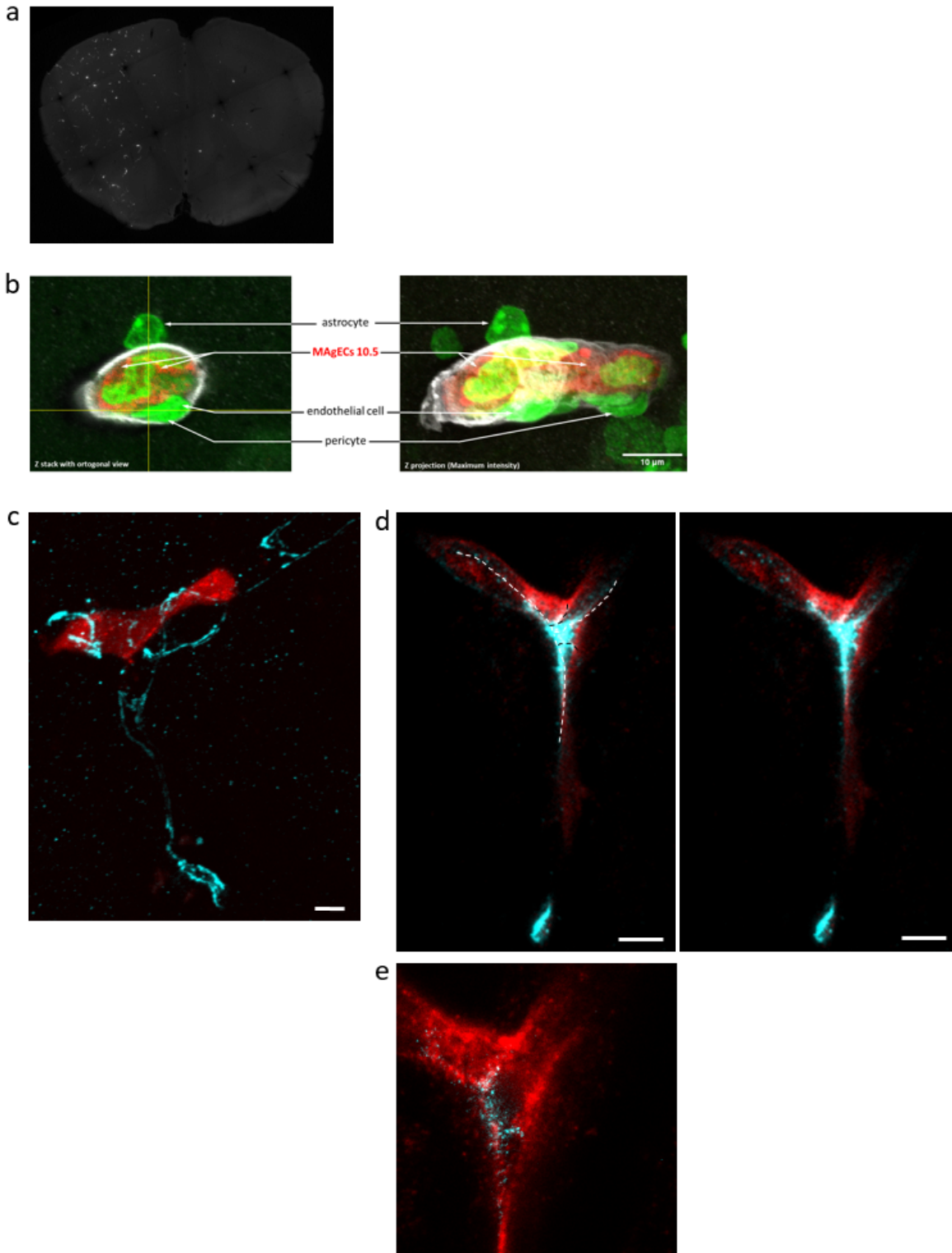


**Figure 5**

**Homing, adhesion and integration of the injected cells into the brain vasculature.** **a**, Detection of the EPCs MAgECs 10.5 labeled by cell tracker red in the brain 4.5 hours after intracarotid injection. Detection on sections of 80 $\mu$ m. The EPCs appear on the sections as white dots. We can see the homing of a fraction of the injected EPCs directly to the brain. **b**, Microscopic detection of the MAgEC 10.5 cells labeled by cell tracker red. Syto 13 (green), which stains all nuclei, permits the approximate identification of the cells by

the position and shape of nuclei. One can identify the astrocytes, the pericytes and the endothelial cells of the vessel wall and the MAgECs inside the vessels. The labeling of collagen IV shows the extracellular matrix and was assessed to identify the relative position of the MAgECs inside the vessels and detect their localisation in the brain microvasculature. **c**, 28 hours after ICA injection of MAgEC 10,5 (Cell tacker red labeled, red), there are EPCs that do not block the brain microvessel lumen completely, hinting at possible integration of the EPC into the vessel wall. The brain capillary is delineated by PECAM-1 immunolabeling (cyan). The image is a maximum intensity projection of a confocal z-stack. **d**, Transduced MAgEC 10,5 RT (tdTomato, immunolabeled with anti-RFP, red) were observed in the brain vasculature 7 days after ICA injection, showing integration into the existing vasculature. The top right capillary branch shows a lumen that appears to be lined with an endothelial cell differentiated from the transduced EPC. The bottom branch appears to contain only partially the red fluorescent cells. Claudin 5 immunolabeling (cyan) shows tight junctions between two edges of the same EPC derived endothelial cell in both upper branches and between an EPC derived endothelial cell (red) and another non labeled endothelial cell (white dashed lines). Between adjacent endothelial cells the tight junction runs the circumference of the vessel sealing the junction of the two cells (black dashed lines), the right panel shows the image without overlay. The image is a maximum intensity projection of a confocal z-stack. **e**, STED image from a single optical section of the stack shown in **d**.) reveals the tight junction strand structure at higher resolution (40 nm pixel size). Bars represent 5  $\mu\text{m}$ .

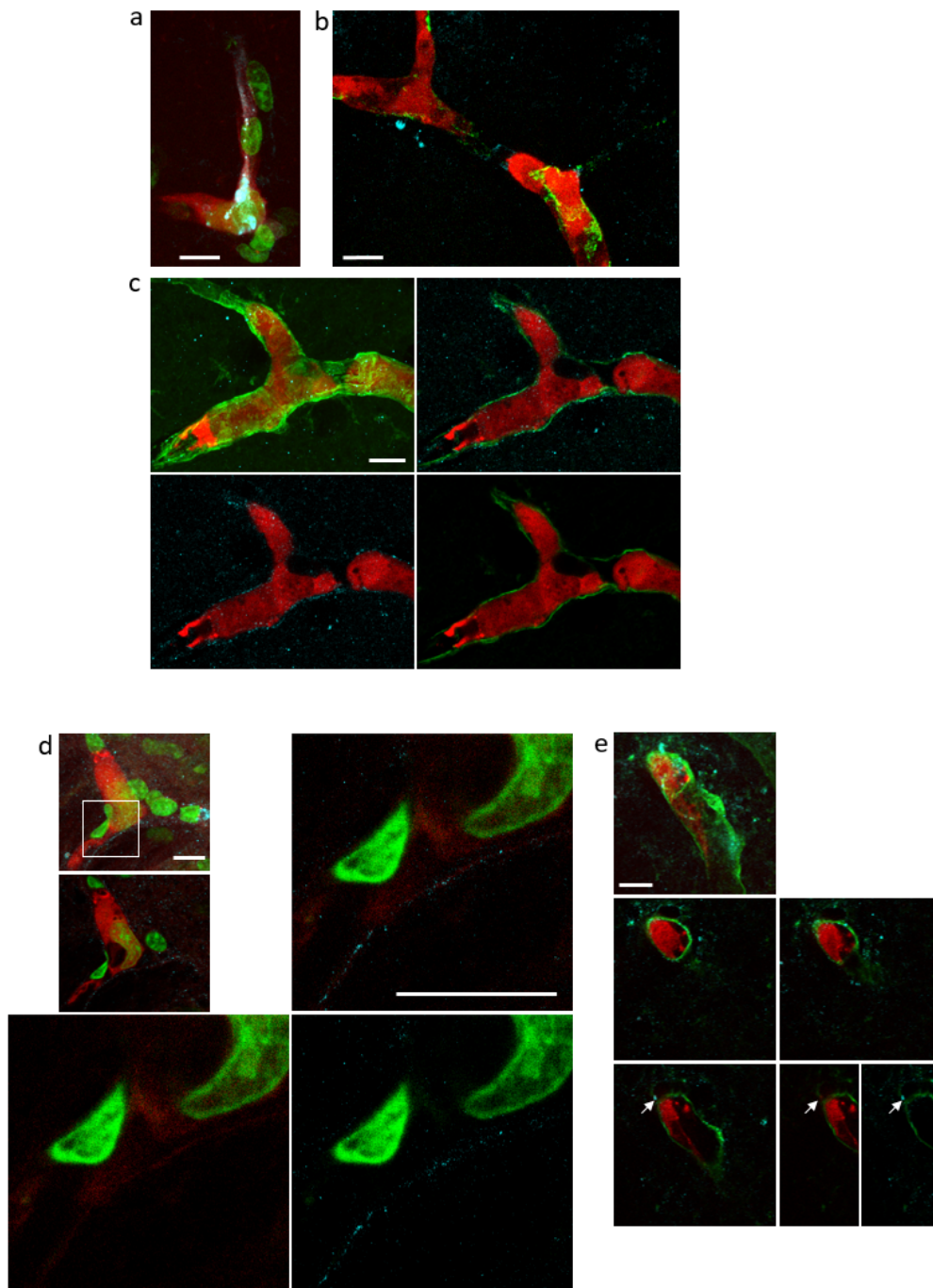


**Figure 6**

**Exogenous TDP-43 antibody secreted by therapeutic MAgEC cells observed in the brain vasculature and brain parenchyma using confocal and super-resolution microscopy.** **a**, MAgEC 10.5 RT anti-TDP-43 cells expressing the fluorescent protein tdTomato (red) and anti TDP-43 Fab fragment (cyan, white in colocalization with red) are discoverable in mouse brain tissue 7 days after intracarotid injection. Nuclear staining (syto-13, green) shows the nuclei of mural cells of a brain microvessel containing MAgEC cells

and that of the MAgEC cells themselves. Maximum intensity projection of confocal images. **b**, Anti-TDP-43 Fab fragments (cyan) produced by MAgEC 10.5 RT anti-TDP-43 cells (red) can pass the blood-brain barrier and localize outside of brain microvessels (labeled using anti-PECAM-1 (green)). Image was taken 48 hours after intracarotid injection. Maximum intensity projection of confocal images. **c**, To further prove that the Fab can penetrate into the brain parenchyma, astrocytic endfeet ensheathing the microvasculature were specifically labeled using antibodies against aquaporin-4 (green). In most brain microvessels observed, the Fab fragments (cyan) secreted by MAgEC 10.5 RT anti-TDP-43 cells (red) localize along the walls of brain microvessels and is spatially indistinguishable from aquaporin-4 labeled astrocytic endfeet surrounding the microvessels on confocal images. First panel shows maximum intensity projection, subsequent panels present a single optical section showing all channels, MAgEC cells and TDP-43 staining, MAgEC cells and aquaporin-4 staining, respectively. **d**, The first two smaller panels present confocal maximum intensity projection and single optical section of a brain microvessel containing MAgEC 10.5 RT anti-TDP-43 cells. In this case aquaporin-4 was stained red to allow simultaneous STED imaging with the TDP-43 Fab (cyan). The larger panels show STED images of the smaller area marked with a white square. On most images it is hard to conclude whether the Fab signal is on the luminal side or the abluminal side of astrocytic endfeet even using super-resolution microscopy. **e**, However, in some cases Fab signal (arrowheads) is clearly localized in the brain parenchyma outside microvessels containing MAgEC 10.5 RT anti-TDP-43 cells. The parenchymal TDP-43 staining, past the aquaporin-4 signal can coincide with red signal from tdTomato originating from MAgEC cells (arrow). The image shows a maximum intensity projection in the first panel, single optical sections in the following panels, the last two panels show aquaporin (green) or TDP-43 (cyan) beside the MAgEC cells.

On all images, the scalebars are 10  $\mu\text{m}$ .

## Supplementary Files

This is a list of supplementary files associated with this preprint. Click to download.

- [Supplementarydata.docx](#)